ARTICLES

Local Structure of CO Coadsorbed with O on Ni(111): A Temperature-Dependent Study†

J.-H. Kang, R. L. Toomes, J. Robinson, and D. P. Woodruff*,‡

Physics Department, University of Warwick, Coventry CV4 7Al, U.K.

R. Terborg, M. Polcik, J. T. Hoeft, P. Baumgärtel, and A. M. Bradshaw§

Fritz-Haber-Institut der Max-Planck-Gesellschaft, Faradayweg 4-6, 14195 Berlin, Germany

Received: July 26, 2000; In Final Form: October 3, 2000

Using C 1s scanned-energy mode photoelectron diffraction (PhD), the local geometry of CO adsorbed onto a Ni(111)(2×2)-O surface has been investigated as a function of the temperature of dosing or subsequent annealing. Around room temperature the CO adopts local atop sites in agreement with the previous interpretation of vibrational spectroscopy, but at low temperature a substantial fraction of the CO molecules adopt the hollow sites occupied in the absence of the preadsorbed O, generally consistent with the results of an earlier PhD study. Heating such a surface leads to a new state in which only atop sites are occupied, but this appears to be a result of desorption of the hollow species rather than any transformation of sites. The results confirm the qualitative site occupations deduced in a recent study of this system which used C 1s and O 1s photoelectron binding energy shifts to fingerprint the local site changes.

1. Introduction

Especially for the case of CO adsorption, vibrational spectroscopy has been used routinely to infer the local adsorption geometry on surfaces. Specifically, a value of the C−O stretching frequency of more than about 2000 cm^{-1} has been taken to imply singly coordinated (atop) adsorption, values in the range of about 1800−2000 cm^{-1} have been associated with 2-fold-coordinated (bridge site) adsorption, and lower frequencies are believed to imply higher (hollow site) coordination.[1] A few years ago a number of truly quantitative structural studies of CO adsorption phases exposed some specific cases in which previous assignments based on these "rules" were found to be incorrect. In particular, the 0.5 monolayer (ML) coverage phase of CO on Ni(111), which forms an ordered c(4×2) phase, had long been interpreted in terms of bridge site adsorption, whereas the true structure was found to comprise equal occupation of the two inequivalent hollow sites, the so-called hcp and fcc sites (directly above Ni atoms in the second and third substrate layers, respectively). The evidence for this revised structural assignment came first from SEXAFS (surface-extended X-ray absorption fine structure) and qualitative LEED (low-energy electron diffraction) arguments[2] and then from a full PhD (scanned-energy mode photoelectron diffraction) study,[3,4] and finally the structure was confirmed using quantitative LEED.[5]

This result, and a small number of similar ones, led to further studies to investigate the extent to which CO vibrational frequency changes associated with coadsorbates may be attributed to site changes. In the case of the Ni(111)/CO system, in particular, the PhD technique was used to investigate the (2×2) surface phases formed by preadsorption of 0.25 ML of either K[6,7] or O.[8] In the case of CO/alkali-metal coadsorption at metal surfaces, there have been many reports of a very large decrease in the C−O stretching frequency, much of which may be associated with a weakening of the C−O bond, although shifts of the adsorbed CO to higher coordination adsorption sites have also been suggested. On Ni(111), however, CO already occupies the highest coordination (hollow) sites even in the absence of coadsorbed K, so the conclusion of the PhD structural study that the same hollow sites are occupied when K is also present on the surface is not especially surprising and does not conflict with the results of vibrational spectroscopy.

In the case of CO/O coadsorption, on the other hand, the PhD study also found CO in the hollow sites whereas a vibrational spectroscopic study of this surface by the group of Yates shows a C−O stretching frequency in the range normally associated with atop adsorption.[9] The implication of this PhD structure determination is thus that the large vibrational shift in the coadsorption case relative to that seen for the pure CO overlayer must be due to a chemical effect rather than a site change. More recently, however, a high-resolution X-ray photoelectron spectroscopy (XPS) study of this system[10] has suggested an alternative interpretation to this apparent inconsistency. In this XPS study a number of different CO adsorption and coadsorption phases on Ni(111) were investigated at different temperatures, and both the C 1s and O 1s XPS peaks showed at least two, and possibly three, distinct chemically shifted states which were attributed to atop, bridge, and hollow adsorption sites. These assignments were based in part on some

† Part of the special issue "John T. Yates, Jr. Festschrift".

* To whom correspondence should be addressed. E-mail: D.P.Woodruff@Warwick.ac.uk. Fax: +44 24 76692016.

‡ Also at Fritz-Haber-Institut der Max-Planck-Gesellschaft.

§ Now at Max-Planck-Institut für Plasmaphysik, Boltzmannstrasse 2, 85748 Garching, Germany.

10.1021/jp0026641 CCC: $20.00
Published on Web 12/15/2000

of the known structures and in part on prior assignments of similar chemical shifts for CO adsorbed on other transition-metal surfaces. In the case of the coadsorption phases it was also assumed that the photoelectron binding energies observed were dependent mainly on the adsorption site and much less on the presence of the coadsorbate. On the basis of this spectral fingerprinting, they concluded that in the Ni(111)(2×2)-O/CO coadsorption phase the CO molecules occupied atop sites if prepared at, or annealed to, around room temperature. If the CO was adsorbed onto the Ni(111)(2×2)-O phase at low temperature, however (corresponding to the conditions of the earlier PhD study), some of the CO molecules appeared to occupy atop sites but others occupied sites of 2- or 3-fold coordination. Heating to 260 K appeared to cause desorption of these high-coordination molecules, leaving only the atop site species.

In view of these XPS results we have undertaken a new PhD study of the Ni(111)(2×2)-O/CO system at different formation temperatures with a view to providing a more quantitative structural understanding of this system. Our new measurements are of the C 1s PhD modulation spectra only, as these are most sensitive to the CO adsorption site, which is the main point of interest. In our structure determination we have conducted an analysis of both the new data and the published data of the previous study using the same methodology. Our final results support the interpretation of the XPS chemical shift fingerprinting, resolve the apparent conflict of the earlier PhD and vibrational spectroscopic studies, and provide a quantitative determination of the associated structural parameters.

2. Experimental Details and Results

The experiments were performed using the established instrumentation and methodology of our many previous PhD adsorbate structural studies [e.g., see ref 11]. The PhD technique exploits the coherent interference between the directly emitted component of the photoelectron wavefield emitted from a core level of an adsorbate atom and components of the same wavefield elastically scattered by the surrounding (mainly substrate) atoms. If the photoemission intensity is measured in a fixed direction as a function of photoelectron energy, the changing photoelectron wavelength causes the scattering paths to move in and out of phase, leading to intensity modulations which are characteristic of the local scattering geometry. The experiments require an intense and tuneable source of incident radiation which, for the present case of a C 1s emission from adsorbed CO, must cover the photon energy range from approximately 360 to 730 eV. This was provided by the HE-TGM1 beamline[12] of the BESSY synchrotron radiation source in Berlin. Installed on this beamline was our UHV surface science end station equipped with a sample manipulator allowing heating and cooling, LEED optics, and a spherical sector electron energy analyzer (VG Scientific, three-channeltron parallel detection) installed at an angle of 60° relative to the incident radiation. The Ni(111) sample was prepared by the usual combination of X-ray Laue alignment, spark machining, polishing, and in situ cycles of argon ion bombardment and annealing until a clean and well-ordered surface was obtained as judged by soft X-ray (synchrotron radiation) XPS and LEED. The initial Ni(111)(2×2)-O surface was prepared by exposing the surface at 300−350 K to 3×10^{-6} mbar·s of oxygen gas followed by briefly annealing to approximately 400 K to yield a sharp (2×2) LEED pattern. CO was then dosed by exposing the surface to approximately 1×10^{-6} mbar·s at 150 K, followed by annealing briefly to 265−270 K, or was similarly dosed at approximately 170 K and measured without any subsequent heating. XPS indicated that the heating treatment led to significant (around 30%) desorption of the original CO coverage.

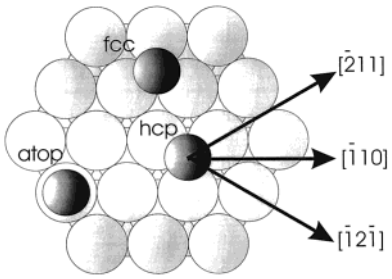

Figure 1. Plan view of a Ni(111) surface showing the atop, hcp hollow, and fcc hollow sites and defining the azimuths used in the data collection.

C 1s PhD spectra were measured at intervals of 10° in polar angle from normal emission to 60°, in each of the three principle high-symmetry azimuths, [$\bar{2}$11], [$\bar{1}\bar{2}\bar{1}$], and [$\bar{1}$10] (Figure 1). For each emission direction a sequence of photoelectron energy distribution curves (EDCs) around the C 1s peak was measured at 2 eV steps in the photon energy over the required range, and these individual EDCs were fitted by the sum of a Gaussian peak, a step, and a template background. The integrated areas of these peaks were then plotted as a function of photoelectron energy, and the final PhD modulation spectrum was obtained by subtraction and normalization by a smooth spline function representing the nondiffractive intensity and instrumental factors. All PhD spectra were measured at low temperature (around 140 K) to reduce the effects of thermal vibrations on the modulation amplitudes. Note that the change produced by annealing a surface initially prepared at low temperature was not reversed on subsequent cooling, indicating that the thermally activated surface transformation was irreversible.

The main purpose of the present study was to characterize the structure of the coadsorption phase after annealing to above 260 K, so the most complete set of data was recorded for this preparation. However, a subset of PhD spectra was also recorded from a lower temperature (170 K) preparation. At first glance the spectra from the two surfaces appeared very similar, although especially at normal emission the modulation intensity seen from the surface which had experienced the 265 K anneal was substantially larger (Figure 2). It was also possible to make a direct comparison of the new data with those obtained in the earlier low-temperature (120 K) investigation for some common directions of emission. Figure 2 shows such a comparison for two key directions, normal emission and 40° emission in the [$\bar{1}\bar{2}\bar{1}$] azimuth. Notice that PhD data recorded in a direction corresponding to 180° scattering by a near-neighbor substrate atom are typically characterized by strong modulations dominated by a single long period associated with the backscattering path from this neighbor. Thus, modulations of this type may be expected at normal emission if the C emitter atom is atop a surface Ni atom, while a C atom occupying an hcp hollow site should show this effect in the [$\bar{1}\bar{2}\bar{1}$] azimuth at a polar emission angle of approximately 40° (see Figure 1). Figure 2 shows rather clearly that the higher temperature surface preparation leads to very strong modulations of this type at normal emission, strongly hinting at an atop adsorption site. On the other hand, the normal emission spectrum recorded in the earlier study at low temperature is quite different; the amplitude of the main features seen at the higher temperature is much smaller, and as a consequence the relative importance of the fine structure is more significant, indicating that at least some of the CO

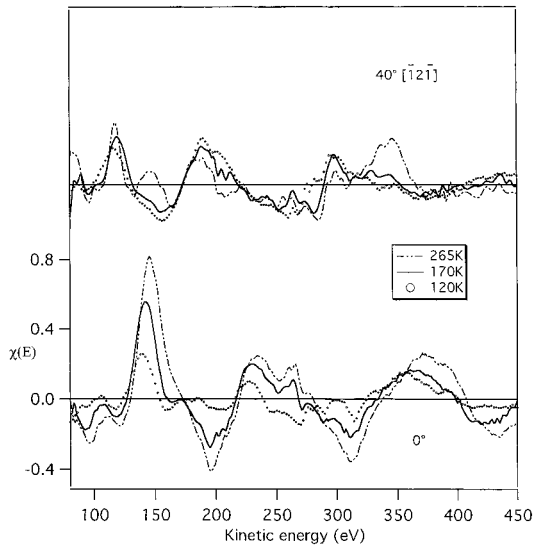

Figure 2. Comparison of the experimental C 1s PhD modulation spectra recorded from the Ni(111)(2×2)-O/CO surface prepared at, or annealed to, three different temperatures. The two emission geometries shown in the comparison are normal emission (the backscatterer direction for atop site occupation) and 40° polar angle emission in the [$\bar{1}\bar{1}2$] azimuth, corresponding approximately to the backscatterer direction for hcp hollow site occupation (see Figure 1). Note that for the normal emission spectra the two new higher temperature data sets were recorded with photon incidence in the [$\bar{1}10$] azimuth, whereas the old data from the 120 K preparation were recorded in the [$\bar{1}2\bar{1}$] azimuth. Past experience of similar adsorption systems indicates that this different polarization direction has relatively little influence on the PhD spectra.

molecules must occupy a different adsorption site. For the off-normal emission geometry, on the other hand, the low-temperature spectrum of the earlier study shows modulations with a single dominant period, consistent with occupation of an hcp hollow site, whereas the 265 K spectrum shows more fine structure. The new "low-temperature" spectra are intermediate between these two extremes, consistent with the fact that the preparation temperature used was itself intermediate between those of the other two data sets.

3. Structure Analysis

While this superficial inspection of a subset of the raw data suggests that the dominant adsorption site of the CO may well change from hcp hollows to atop as the preparation temperature increases, a more quantitative analysis of the PhD data is clearly required. We achieve this in two stages.[11] First, we apply the "projection method" of direct data inversion[13,14] to obtain an approximate "image" of the scattering atoms around the emitter. The method exploits the fact that, especially in the near-backscattering geometry from near neighbors, the PhD spectra are dominated by the single scattering pathway from this neighbor, so calculating the projection of the experimental data onto single scattering simulations for a single neighbor in different possible positions leads to peaks at positions corresponding to the actual locations of such neighbors. The resulting images can commonly provide a first-order estimate of the local adsorption site and associated bond lengths.

The results of applying this method to the three different PhD data sets leads to the results summarized in Figure 3 in the form of gray-scale maps of sections of space around the emitter (located at (0,0,0)). The darkest regions correspond to the highest values of the projection integral and thus the most probable location of backscattering atoms. On the left are shown sections

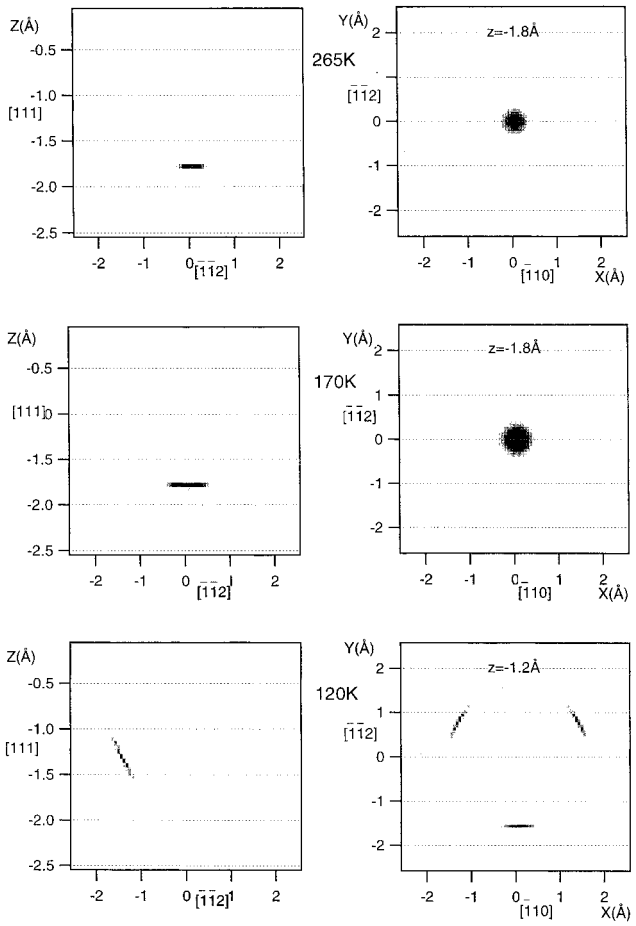

Figure 3. Results of applying the "projection method" of direct data inversion to the C 1s PhD modulation spectra collected at the three different surface preparation or annealing temperatures of the Ni(111)-(2×2)-O/CO phase. Data from the lowest temperature preparation are taken from the earlier published study.[8] Each panel comprises a gray-scale map of the projection parameter, which is expected to be largest (and thus darkest in the map) at the positions most likely to correspond to the locations of near-neighbor Ni backscatterer atoms. On the left are shown cuts in three-space perpendicular to the surface and passing through the emitter at (0,0,0). On the right are cuts parallel to the surface at depths chosen to intersect the peaks seen in the perpendicular sections.

perpendicular to the surface in the [$\bar{1}\bar{1}$2] azimuth (equivalent to the [$\bar{1}2\bar{1}$] azimuth). At the two higher temperatures these sections are dominated by a single feature approximately 1.8 Å below the emitter, and sections parallel to the surface at this depth (shown on the right-hand side) clearly show this one backscatterer image directly below the emitter, consistent with an atop adsorption site. For the lowest temperature data, on the other hand, the section perpendicular to the surface shown on the left has a feature 1.2 Å below the emitter but offset by more than 1 Å to the side. In this case the section parallel to the surface through this peak shows three equivalent features consistent with the three nearest-neighbor Ni atoms of an emitter in an hcp hollow site (cf. Figure 1). These projection method maps thus provide further confirmation of a probable atop geometry for the higher temperatures and hcp hollow site adsorption at the lowest temperature. Of course, the projection method is not only approximate in locating backscatterer atom positions, but is also designed only to locate the strongest scatterer contributions. These results therefore do not necessarily imply that *only* the atop site is occupied at the higher temperatures, nor that *only* hcp sites are occupied at the lowest temperatures.

To obtain a fully quantitative structural analysis, we therefore make use of an iterative "trial-and-error" procedure which involves a comparison of usually 4−8 experimental spectra with the results of multiple scattering simulations based on trial model structures. These calculations are performed with codes developed by Fritzsche[15,16] which are based on the expansion of the final state wave function into a sum over all scattering pathways which the electron can take from the emitter atom to the detector outside the sample. A magnetic quantum number expansion of the free electron propagator is used to calculate the scattering contribution of an individual scattering path. Double and higher order scattering events are treated by means of the reduced angular momentum expansion (RAME). The finite energy resolution and angular acceptance of the electron energy analyzer are accounted for analytically. Anisotropic vibrations for the emitter atom and isotropic vibrations for the scattering atoms are also taken into account. The comparison between theoretical and experimental modulation amplitudes, χ_{th} and χ_{ex}, is quantified by the use of a reliability factor

$$R_m = \sum(\chi_{th} - \chi_{ex})^2 / \sum(\chi_{th}^2 + \chi_{ex}^2) \quad (1)$$

where a value of 0 corresponds to perfect agreement, a value of 1 to uncorrelated data, and a value of 2 to anticorrelated data. The search in parameter space to locate the structure having the minimum *R* factor was performed with the help of an adapted Newton−Gauss algorithm and an approximate "linear" version of the multiple scattering code in the initial searches.[17] To estimate the errors associated with the individual structural parameters, we use an approach based on that of Pendry which was derived for LEED.[18] This involves defining a variance in the minimum of the *R* factor, R_{min}, as

$$\mathrm{var}(R_{min}) = R_{min}(2/N)^{1/2} \quad (2)$$

where *N* is the number of independent pieces of structural information contained in the set of modulation functions used in the analysis. All parameter values giving structures with *R* factors of less than R_{min}+ var(R_{min}) are regarded as falling within 1 standard deviation of the "best-fit" structure. More details of this approach, in particular on the definition of *N*, can be found in a recent publication.[19] Note that the precision in an individual parameter is usually determined by investigating the change in R_m with this parameter alone, an approach which neglects any possible role of coupling between two or more parameters. In the present case checks revealed there were no instances of strong coupling of this kind.

The initial stages of full structure analysis concentrated on the new data associated with the higher temperature preparation of the surface, but subsequently a similar analysis was performed on the new low-temperature data, and finally, to ensure a consistent methodology, the old (previously published) lower temperature data were reanalyzed. In all cases the first models to be tested were those based on occupation of a single high-symmetry site, namely, atop, hcp hollow, or fcc hollow (being, respectively, atop Ni atoms in the first, second, and third layers of the substrate). In each case the main parameter varied was the spacing of the C atom in the CO to the outermost Ni layer, z_{C1}. Additional parameters explored included the vibrational amplitudes of the emitter and scatterer atoms, and various local relaxations of the substrate, notably in the spacing of the outermost Ni layer and in the second-layer rumpling. It became clear, however, especially with the later consideration of multiple-site occupancy, that the large number of structural variables not only hugely increased the computational complexity, but more importantly allowed convergence on unphysical solutions involving huge subsurface rumpling. One reason for this is that PhD is intrinsically a very local technique and is rather insensitive to the exact positions of atoms which are not near neighbors; for example, for adsorption in an hcp site the PhD spectra are quite sensitive to the position of the second-layer Ni atom directly below the emitter, but rather insensitive to the position of the neighboring atoms in this layer. Even though an unphysically large rumpling of this layer may improve the *R* factor, this improvement is too small to be statistically significant, so including this possibility does not provide a more meaningful analysis. Subsequent fitting therefore concentrated on an ideally terminated Ni(111) substrate.

TABLE 1: Summary of the Best-fit Structural Parameters for CO in the Ni(111)(2×2)-O/CO Phase for Different Preparation or Annealing Temperatures[a]

preparation or annealing temp (K)	proportion of atop sites (%)	C−Ni layer spacing (atop) (Å)	C−Ni layer spacing (hcp hollow) (Å)
265	95 (+5/−25)	1.77 ± 0.02	1.26*
170	70 ± 20	1.79 ± 0.03	1.28 ± 0.12
120	35 (+20/−25)	1.81 ± 0.08	1.29 ± 0.04

[a] In all cases the structures are a mixture of atop and hcp hollow site occupation. In the case of the data from the surface annealed at 265 K, the fits showed an extremely weak dependence on the C−Ni layer spacing for the hcp site because of the very low fractional occupation of this site, so no error limits could be established by the standard approach described in the text.

In the case of the two new data sets associated with annealing or preparation temperatures of 265 and 170 K, the best fits based on single-site occupancy were for atop sites, with *R* factor values of 0.23 and 0.31, respectively. A similar single-site fit to the older data based on a surface preparation at 120 K favored hcp site occupation with an *R* factor of 0.35. Typically in PhD, *R* factor values in the range 0.2−0.3 represent "good" fits to the data, although in simple structures values as low as 0.1 or less have sometimes been achieved. Further structural optimization was then performed by considering models based on mixed-site occupancy, and specifically occupation of both atop and hcp sites. Note that this mixture was clearly favored relative to fcc and atop. A number of tests were conducted involving the possibility of occupation of atop, hcp hollows, *and* fcc hollows, but these indicated that any fcc site occupation causes an increase in the *R* factor; more than about 10% fcc site occupation typically shifts the *R* factor outside the variance for the best-fit structure, so any fcc site occupation can only occur as a minor component. These mixed-site calculations are time-consuming because it is necessary to optimize the geometry of each component site at each mixture. Such a procedure is generally important, because if data are collected from a mixture of sites, there is no reason to believe that the geometry of an optimized single-site fit is the correct geometry for this site in a multisite fit. In fact, having established the optimal multisite structural parameters in the present case, checks were conducted on the possibility of a coupling between the parameter describing the relative site occupancy and the primary structural parameters of the individual sites, but no significant coupling was found. Moreover, these geometries are essentially the same as those found for the optimized single-site fits. This is not entirely surprising because the lowest and highest temperature preparations do correspond to the majority of the CO molecules in single sites.

The main results of this fitting procedure are summarized in Table 1 and in Figures 4 and 5. The actual best-fit structural parameter values are shown in Table 1, while comparisons of

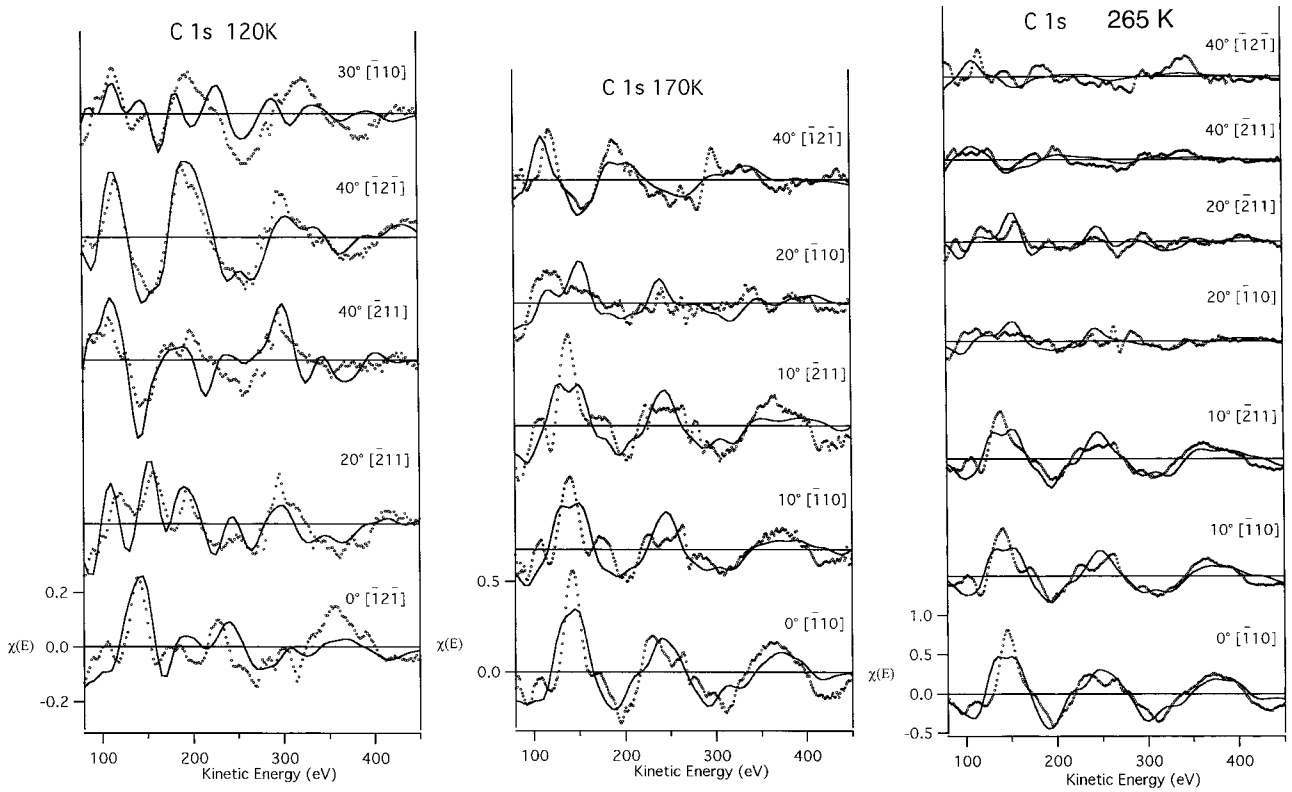

Figure 4. Comparison of the calculated C 1s PhD modulation spectra (full lines) from the best-fit structural models for the CO adsorption geometry (see Table 1) with the experimental data (circles) for the three different surface preparation or annealing temperatures of the Ni(111)(2×2)-O/CO phase. Data from the lowest temperature preparation are taken from the earlier published study[8] but are shown here over the same (slightly shorter) energy range used for the new data.

the results of these fits with the experimental data are shown in Figure 4. Figure 5 shows the dependence of the quality of the fits, as determined by the *R* factor, on the fractional occupation of the two sites. This figure shows rather clearly that at the highest temperature the optimal fit corresponds to almost pure atop site occupation, with only a marginal improvement effected by the inclusion of 5% occupation of the hcp hollow site. By contrast, *any* addition of fcc site occupation leads to an increase in the *R* factor. Even the lowest temperature preparation leads to PhD data which are fitted significantly better (the *R* factor falling from 0.35 to 0.27) by a model not based on pure hcp hollow site occupation, but rather with some 35% atop site occupation. A similar improvement occurs for the intermediate temperature data if the pure atop site model is replaced by one including 30% hcp hollow site occupation.

4. General Discussion and Conclusions

The overall structural conclusions summarized in Table 1 clearly reconcile previous studies of the Ni(111)/O/CO coadsorption system aimed at determining in a quantitative or qualitative fashion the local adsorption geometry of the CO. As suggested by the high-resolution XPS study,[10] CO adopts atop sites in the presence of coadsorbed O when the surface is formed at around room temperature, whereas if the surface is prepared at sufficiently low temperature a large fraction of the CO molecules occupy the hollow sites as they do in the absence of preadsorbed O. At first sight this implies a puzzling irreversible site change as the surface is heated. However, more careful consideration of the results of the original vibrational spectroscopic study by Yates and co-workers[9] provides an alternative interpretation. In this study the role of the exact precoverage of oxygen was investigated carefully, and it was found that while a coverage of exactly 0.25 ML (the ideal value for a perfect (2×2)-O phase) appeared to indicate only atop adsorption, even at 90 K, different (especially lower) predoses led to spectra indicative of co-occupation of more highly coordinated sites. Moreover, as also noted in the XPS study of Held et al.,[10] heating a surface prepared at low temperature led to preferential desorption of this more highly coordinated species. The fact that in both our study and that of Held et al. partial desorption was observed on annealing thus strongly indicates that in both of these studies the oxygen predose we used was not exactly 0.25 ML, and that regions of the surface were probably depleted of oxygen, allowing occupation of the hollow sites. Moreover, comparison of the relative oxygen precoverages in the present low-temperature PhD study and the earlier one of Fernandez et al.,[8] as judged by the O and Ni XPS signal ratio, indicates that the earlier study used a significantly lower oxygen precoverage than in the present work, thus allowing more hollow site occupation. The key difference between these two low-temperature studies is therefore probably not the exact preparation temperature, but the magnitude of the oxygen precoverage. With this understanding our data present a far more straightforward picture in which we infer that well-ordered (2×2)-O regions do involve only atop CO species, but at lower temperatures hcp CO may be coadsorbed on regions of the surface with a lower local O coverage.

There remain, however, a few questions. One concerns the detailed results of the previous PhD study which concluded that the low-temperature preparation led to occupation of *both* hcp and fcc hollow sites (but with a higher fraction—70%—in the hcp sites), whereas the present reanalysis of the PhD spectra from this earlier study favors a mixture of hcp sites (essentially the same fractional value of 65%) and atop sites. A key reason

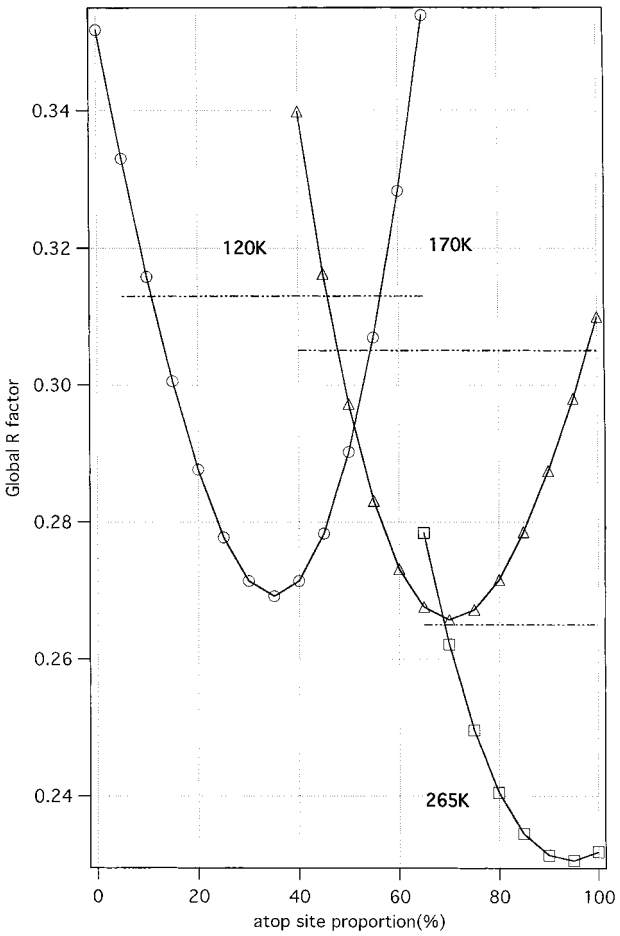

Figure 5. Graph showing the dependence of the *R* factor on the relative proportion of atop and hcp hollow site occupation for the adsorbed CO molecules in the Ni(111)(2×2)-O/CO surface prepared at or annealed to the three different temperatures. The dashed lines parallel to the abscissa correspond to the values (R_{min} + var(R_{min})) for each data set and define the estimated precision.

for this is that because of the strong similarity of the off-normal emission data to those found in the absence of preadsorbed O and the fact that the projection method clearly identified the hollow site, the possibility of partial occupation of atop sites was not properly explored. Of course, neither the visual inspection of the data nor the direct data inversion approach is particularly sensitive to minority species. A second point of significance, however, concerns the choice of the spectral data set used in the quantitative analysis. In general, our strategy for choosing the subset of spectra used in the structure analysis by PhD has been to attempt to select a reasonable range of emission angles, yet to concentrate on those showing the strongest modulations. Emission directions corresponding to strong modulations certainly include the main backscatterer directions and thus provide the best precision in the determination of the near-neighbor distances and the adsorption site. Strong modulations also ensure that the effects of experimental noise and artifacts, and indeed of any weaknesses in the theoretical treatment, have the least effect on the analysis, rendering the results more precise.

In the case of co-occupation of two (or more) sites, however, each site will contribute modulations most strongly in different directions, and if the data set is biased toward data close to one of these directions, the analysis may favor this adsorption geometry. In the present case, the new data sets used in the analysis are somewhat weighted toward near normal emission (one spectrum at 0° and two each at 10°, 20°, and 40°), favoring the atop site backscattering detection, whereas the original low-temperature data set was less weighted in this way (0°, 20°, 30°, and two at 40°). Of course, this choice reflects largely the fact that at the lowest temperature the majority occupation is the hollow sites and at the higher temperatures it is the atop sites. Nevertheless, it is notable that if one looks at the dependence of the *R* factors calculated for individual emission spectra as a function of relative site occupation (i.e., the plot equivalent to that of Figure 5), one finds that for both the lower temperature data sets the spectra recorded near normal emission favor atop site occupation and those far from normal emission favor hollow site occupation. This is entirely to be expected, yet it highlights the fact that the choice of data set may influence the best combination of sites to minimize the global (multi-spectral) *R* factor. An important factor ameliorating this problem is that the *R* factor does weight most strongly the spectra with the largest modulation amplitudes (see eq 1), so providing the data set includes the backscattering directions for all the sites, these spectra should dominate the optimization.

Beyond this rather technical matter, however, one key conclusion we can draw from this new study, combined with the results of the original vibrational spectroscopy investigation of Yates and co-workers, is that CO adsorption on an ideal (2×2)-O surface almost certainly is entirely in atop sites. However, these studies also provide a reminder that the observation of a good (2×2) LEED pattern does not guarantee that the whole surface comprises this well-ordered adsorbate phase. The partial occupation of hcp sites at low temperatures appears to reflect the availability of regions of the surface which are depleted in oxygen, although whether this is in the form of bare islands or local oxygen vacancies is unclear; the fact that only hcp sites are occupied seems to favor the latter interpretation, as bare islands would be expected to show both hcp and fcc site occupation. A somewhat similar problem is raised by the implication of the high-resolution XPS study that even for the Ni(111)c(4×2)-CO structure,[10] which is well-established to comprise one hcp hollow CO and one fcc hollow CO per primitive surface unit mesh at low temperature, partial occupation of atop (and possibly bridge) sites occurs at room temperature. Clearly in this case too either the structure is not perfectly long-range-ordered, and local fluctuations in geometry occur, or the well-ordered regions giving the LEED pattern cover only part of the surface.

Acknowledgment. This work was supported by the German Federal Ministry of Education, Science, Research and Technology (Contract No. 05 625EBA 6), by the Fonds der Chemischen Industrie, by the European Community HCM program through Large Scale Facilities support to BESSY, and by the Physical Sciences and Engineering Research Council (U.K.) in the form of a research grant and a Senior Research Fellowship for D.P.W.

References and Notes

(1) Sheppard, N.; Nguyen, N. T. *Adv. IR Raman Spectrosc.* **1978**, *5*, 67.

(2) Becker, L.; Aminpirooz, S.; Hillert, B.; Pedio, M.; Haase, J.; Adams, D. L. *Phys. Rev. B* **1993**, *47*, 9710

(3) Schindler, K.-M.; Hofmann, Ph.; Weiss, K.-U.; Dippel, R.; Fritzsche, V.; Bradshaw, A. M.; Woodruff, D. P.; Davila, M. E.; Asensio, M. C.; Conesa, J. C.; Gonzalez-Elipe, A. R. *J. Electron Spectrosc. Relat. Phenom.* **1993**, *64/65*, 75.

(4) Davila, M. E.; Asensio, M. C.; Woodruff, D. P.; Schindler, K.-M.; Hofmann, Ph.; Weiss, K.-U.; Dippel, R.; Gardner, P.; Fritzsche, V.; Bradshaw, A. M.; Conesa, J. C.; González-Elipe, A. R. *Surf. Sci.* **1994**, *311*, 337.

(5) Mapledoram, L. D.; Bessent, M. P.; Wander, A. D.;.King, D. A. *Chem. Phys. Lett.* **1994**, *228*, 527.

(6) Davis, R.; Woodruff, D. P.; Schaff, O.; Fernandez, V.; Schindler, K.-M.; Hofmann, Ph.; Weiss, K.-U.; Dippel, R.; Fritzsche, V.; Bradshaw, A. M. *Phys. Rev. Lett*. **1995**, *74*, 1621.

(7) Davis, R.; Toomes, R.; Woodruff, D. P.; Schaff, O.; Fernandez, V.; Schindler, K.-M.; Hofmann, Ph.; Weiss, K. U.; Dippel, R.; Fritzsche, V.; Bradshaw, A. M. *Surf. Sci*. **1997**, *393*, 12.

(8) Fernandez, V.; Schindler, K.-M.; Schaff, O.; Hofmann, Ph.; Theobald, A.; Bradshaw, A. M.; Fritzsche, V.; Davis, R.; Woodruff, D. P. *Surf. Sci*. **1996**, *351*, 1.

(9) Xu, Z.; Surnev, L.; Uram, K. J.; Yates, J. T. Jr., *Surf. Sci.* **1993**, *292*, 235.

(10) Held, G.; Schuler, J.; Sklarek, W.; Steinrück, H.-P. *Surf. Sci.* **1998**, *398*, 154.

(11) Woodruff, D. P.; Bradshaw, A. M. *Rep. Prog. Phys.* **1994**, *57*, 1029.

(12) Dietz, E.; Braun, W.; Bradshaw, A. M.; Johnson, R. L. *Nucl. Instr. Meths. A* **1985**, *239*, 35.

(13) Hofmann, Ph.; Schindler, K.-M. *Phys. Rev. B* **1993**, *47*, 13941.

(14) Hofmann, Ph.; Schindler, K.-M.; Bao, S.; Bradshaw, A. M.; Woodruff, D. P. *Nature* **1994**, *368*, 131.

(15) Fritzsche, V. *J. Phys.: Condens. Matter* **1990**, *2*, 1413; *Surf. Sci*. **1992**, *265*, 187.

(16) Fritzsche, V. *Surf. Sci*. **1986**, *213*, 648.

(17) Fritzsche, V.; Pendry, J. B. *Phys. Rev. B* **1993**, *48*, 9054.

(18) Pendry, J. B. *J. Phys. C: Solid State Phys.* **1980**, *13*, 937.

(19) Booth, N. A.; Davis, R.; Toomes, R.; Woodruff, D. P.; Hirschmugl, C.; Schindler, K.-M.; Schaff, O.; Fernandez, V.; Theobald, A.; Hofmann, Ph.; Lindsay, R.; Gieâel, T.; Bradshaw, A. M. *Surf. Sci*. **1997**, *387*, 152.